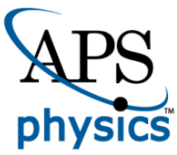

This is the accepted manuscript made available via CHORUS. The article has been published as:

First Six Dimensional Phase Space Measurement of an Accelerator Beam

Brandon Cathey, Sarah Cousineau, Alexander Aleksandrov, and Alexander Zhukov

Phys. Rev. Lett. **121**, 064804 — Published 10 August 2018

DOI: 10.1103/PhysRevLett.121.064804

First Six Dimensional Phase Space Measurement of an Accelerator Beam*

Brandon Cathey and Sarah Cousineau†
Department of Physics and Astronomy, University of Tennessee, Knoxville Tennessee 37966, USA

Alexander Aleksandrov and Alexander Zhukov
Oak Ridge National Laboratory, Oak Ridge, Tennessee 37831, USA
(Dated: June 25, 2018)

This paper presents the first complete six-dimensional phase space measurement of a beam in an accelerator. The measurement was made on the Spallation Neutron Source (SNS) Beam Test Facility (BTF). The data reveals previously unknown correlations in the 6D phase space distribution that are not visible in lower dimensionality measurements. The correlations are shown to be intensity dependent.

The field of accelerator physics relies heavily on particle tracking simulations for the study of beam dynamics in an accelerator. Currently, a significant limitation is the inability of simulation tools to accurately predict the beam distribution in a hadron linear accelerator. Even state-of-the-art particle-in-cell codes that contain all the relevant physics are only able to reproduce the beam's measured root-mean-square (RMS) parameters. However, characterizing the beam at several sigma beyond RMS is necessary to predict beam loss [1]. The discrepancy is believed to stem from a poor understanding of the actual initial distribution [2–6], which fundamentally limits the extent to which simulation tools can aid in the optimization and the design of current and future accelerators.

Modern day hadron linear accelerators are composed of a radio frequency quadrupole (RFQ) followed by a series of accelerating cavities designed for progressively higher energies that together constitute a linac. Because linacs are not a closed loop, the beam dynamics throughout are intimately dependent on the initial beam entering the system. There are three components required to accurately simulate a linac: the physics of the accelerating and transport devices, the Coulomb forces between charges, and the phase space particle distribution of the beam entering the linac. The accelerator community agrees that the physics of the transport devices and the Coulomb forces are accurately represented within simulations. As mentioned above, they also agree that the discrepancy with measurement stems from the lack of having an accurate full six-dimensional phase space distribution of a hadron beam in a linac. Logically, without knowing this distribution, there should be no expectation that simulations will accurately predict the beam evolution.

A particle in an accelerator is described by six independent degrees of freedom. In a Cartesian coordinate system, they are: the horizontal and vertical positions and their conjugate momentum $(x, x' = p_x/p_z, y, y' = p_y/p_z)$, and the energy and phase relative to a design reference particle (w, φ). Thus, a beam is fully described by its distribution of particles in the 6D phase space, and complete measurement of a distribution must include all six dimensions and their cross-correlations. Unfortunately, traditional beam diagnostics only measure projections of the phase space in one, two, or at most four dimensions. Typically, 2D projections of corresponding position and momentum distribution functions $f_{\mathrm{x}}(x, x')$, $f_{\mathrm{y}}(y, y')$, $f_{\mathrm{z}}(w, \varphi)$, customarily called emittances, are measured independently [7]. To create an initial 6D distribution f_6 for simulations, these 2D projections are assembled together with the assumption that there are no correlations between the degrees of freedom not explicitly measured simultaneously:

$$f_6 = f_{\mathrm{x}}(x, x') \cdot f_{\mathrm{y}}(y, y') \cdot f_{\mathrm{z}}(w, \varphi) \tag{1}$$

This equation is the definition of uncorrelated distributions f_{x}, f_{y}, f_{z} and is only true if the degrees of freedom are independent. However, existing experimental measurements do not support this assumption. Simple linear correlations between transverse dimensions were demonstrated by measuring RMS beam parameters [8]. Beyond this, complex correlations have been measured between the transverse RMS parameters and longitudinal coordinates for electron beams through the slice emittance technique [9]. Therefore, Eq (1) is not valid in general, and a direct measurement of the full 6D phase space is required to obtain an accurate distribution for realistic simulations. Specific correlations are known to affect beam evolution [10, 11], and undiscovered correlations could further influence beam dynamics.

There have been previous high dimensionality measurements. "Pepper-pot" methods have demonstrated direct transverse distribution measurements up to 4D [12]. A variety of tomographic techniques have also been developed to reconstruct higher dimensionality distributions using lower dimensionality projections. In general, the techniques are used to reconstruct transverse or longitudinal 2D projections of the 6D distribution using measured 1D projections [13–17], or in one case to reconstruct the 4D transverse distribution from 1D spatial profiles [18]. The full six-dimensional measurement has not been achieved until this point.

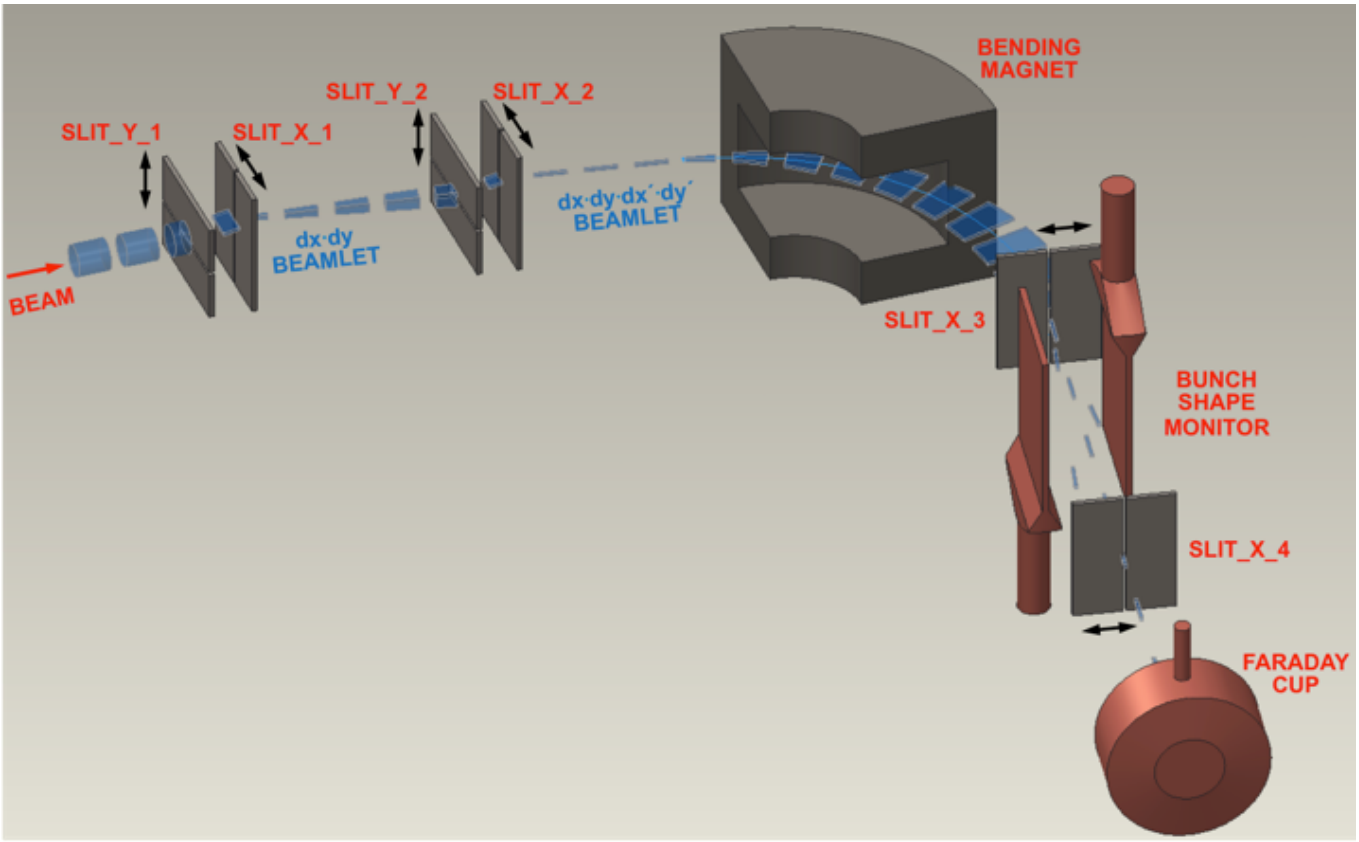

FIG. 1. A diagram showing the principle behind a full six dimensional emittance scan.

A straightforward method for measuring the 6D phase space distribution of a beam was proposed in [19]. Figure 1 illustrates the principle of the method. A set of six movable slits is used to localize particles inside a small area of the 6D phase space: the first pair of orthogonal slits transmits only particles with coordinates within intervals $x \pm \Delta x$, $y \pm \Delta y$; the second pair of orthogonal slits at a set distance from the first pair transmits only particles with angles within intervals $x' \pm \Delta x'$, $y' \pm \Delta y'$; the fifth slit, placed at a location with large energy dispersion created by a bending magnet, transmits only particles with energy within interval $w \pm \Delta w$. The remaining particles pass through an RF deflector, which deflects particles in accordance with their time of arrival. Only particles with arrival phases within interval $\varphi \pm \Delta\varphi$ are transmitted through the sixth slit. At the end, particles within the interval $\pm(\Delta x \Delta x' \Delta y \Delta y' \Delta w \Delta\varphi)$ around the point $(x, x' y, y', w, \varphi)$ in the 6D phase space are collected by a Faraday cup, and their total charge is measured. The fraction of particles inside the interval is small: only about one in ten million particles will reach the Faraday cup when measuring the beam core. The distribution function is measured by moving all the slits sequentially to span the whole phase space occupied by the beam. As the scan is sequential, it requires n^6 steps, where n is the number of points per each dimension. In practice, a multi-hour scan is required to achieve a reasonable resolution of 10-20 points per dimension. Therefore, the technique is ideally suited for a dedicated facility with significant beam time available for measurement.

This technique was implemented at the SNS Beam Test Facility (BTF), which is a functional duplicate of the SNS linac injector [20]. The BTF is capable of producing a pulsed 2.5MeV H^- ion beam with a peak current of up to 50mA, pulse width of 50μs, and repetition rate of 10Hz when using the beam line diagnostics. The typical transverse RMS emittance is 0.4mm·mrad; the longitudinal emittance is approximately 0.25MeV·deg at 402.5MHz. The 6D scan hardware design closely followed the Fig.1 concept: the four transverse slits have 200μm wide apertures, the transverse slit pairs are 0.94m apart, the bend angle is 90°, and the energy slit is 800μm wide. The bending magnet also guarantees any H^+ caused from edge scattering will not disrupt the final charge measurement.

The largest difference from the concept is the last stage. Deflecting the 2.5MeV H^- ions would require inconveniently large RF power, and therefore the temporal degree of freedom was instead measured by analyzing the time of arrival of secondary electrons produced when the H^- ions strike a tungsten wire in the beam path [21]. Also, in order to reduce the scan time, the last slit

was replaced by a luminescent screen and video camera, the linearity and accuracy of which was checked against a Faraday cup, so that the whole temporal profile was measured in one pulse. The detailed description of the experiment hardware, 6D scan implementation, and data analysis will be published separately.

Many measurements, including the first full six-dimensional scan, were completed using the technique described above. The six-dimensional scan took 32 hours and resulted in 5,675,740 points on a near-regular grid in the 6D phase space. Figure 2 shows that the beam current during the 6D scan, measured upstream of the slits, remained constant for the duration except for a few dropouts. Measurements throughout the year the BTF was operational remained consistent, including higher dimensional data verified by trusted lower dimensional data. These data can be used to generate an input set of particle initial coordinates for computer simulations, but higher resolution is desirable for an accurate simulation. More importantly, the experimental data provide an opportunity to explore the internal structure of the full phase space distribution, and specifically to check for correlations between coordinates in all six degrees of freedom. There is no proven technique for finding arbitrary correlations in high-dimensional spaces. The linear correlation coefficients can be calculated for all combinations of the six degrees of freedom, but even zero values for the correlation coefficients do not guarantee the absence of higher order correlations, and a correlation of any order invalidates equation (1). Full exploration of this problem remains to be done.

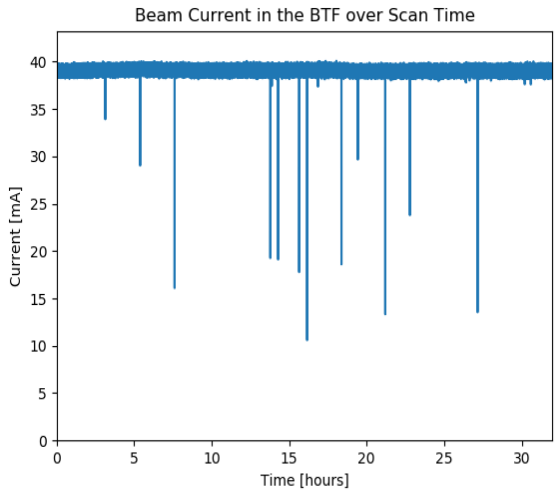

FIG. 2. The beam current upstream of the slits measured during the 6D scan.

As a first step, a visual inspection of various 1D and 2D projections and partial projections of the 6D distribution was conducted. The key advantage of using the partial projections is that they avoid integration over all dimensions, which can mask important details of the high dimensionality distribution. The following definitions are used in the data analysis discussion below. Full projections are reduced dimensionality distribution functions obtained by integrating over all unused coordinates:

$$1D : f(a) = \int_{-\infty}^{\infty} f_6(a, \vec{x}) d\vec{x} \tag{2}$$

$$2D : f(a, b) = \int_{-\infty}^{\infty} f_6(a, b, \vec{x}) d\vec{x} \tag{3}$$

On the other hand, partial projections are reduced dimensionality distribution functions obtained by fixing some coordinates to constant values and integrating over others:

$$1D : p(a) = \int_{-\infty}^{\infty} f_6(a, \vec{v} = \vec{v}_0, \vec{x}) d\vec{x} \tag{4}$$

$$2D : p(a, b) = \int_{-\infty}^{\infty} f_6(a, b, \vec{v} = \vec{v}_0, \vec{x}) d\vec{x} \tag{5}$$

In the formulas above, a, b are any coordinate from the $(x, x'y, y', w, \varphi)$ set; $\vec{v}$ is a vector of coordinates remaining in the $(x, x'y, y', w, \varphi)$ set after a, b are removed; $\vec{x}$ is the vector of coordinates remaining in the $(x, x'y, y', w, \varphi)$ set after a, b and $\vec{v}$ are removed. Vector $\vec{v}$ is equal to the vector $\vec{v}_0$, which is the fixed coordinate of interest for the partial projection. A partial projection can be measured directly by leaving the slits responsible for fixed coordinates at fixed positions. These scans are much faster than full 6D scans and allow exploring identified correlations with higher resolution. Multiple scans with different beam parameters can also be done this way in reasonable time durations.

A clearly visible correlation was found between the transverse degrees of freedom and the energy. Figure 3 shows a 2D color map of the $p(x', w)$ partial projection with $x = y = y' = 0$ (these slits were fixed in the beam center while the x' slit was allowed to move) and integrated over φ (the wire was removed from the beam path). A dependence of the w distribution upon the coordinate value x' is obvious in the plot. The w distribution showed similar dependence with x, y, and y' as well.

The multi-dimensional nature of the observed correlation is illustrated in Fig. 4 with plots derived from a 5D scan with integration over φ. Several 1D partial projections for different values of x' are plotted on the right. A full projection on the energy axis (i.e. the energy spectrum) is plotted on the left. The full beam energy spectrum projection does not show any hint of

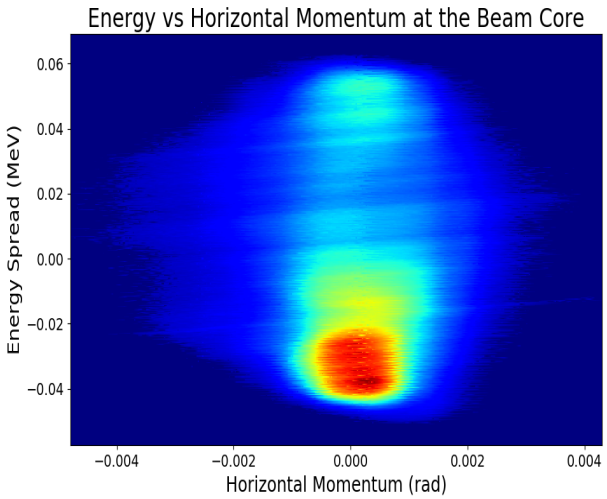

FIG. 3. A partial projection plot of the energy spread w against the horizontal momentum x'.

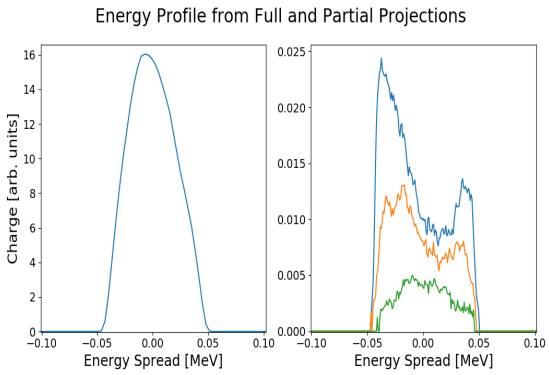

FIG. 4. Results from a 5D scan. The left plot shows the total projection of the energy spectrum. The right shows different 1D partial projections of energy with three different horizontal momentums. The blue curve's x' is about 0.2mrad, yellow's is about 0.7mrad, and green's is about 1mrad.

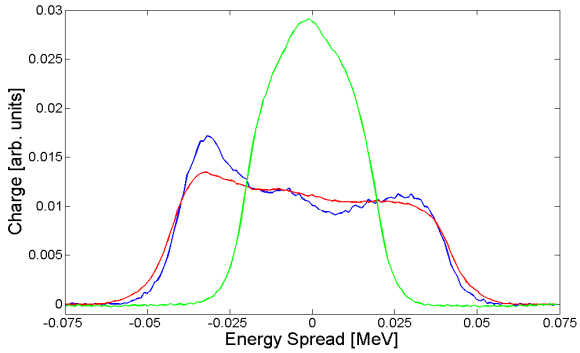

FIG. 5. Plots of three different 1D partial projections on energy. Each plot has a different number of fixed slits near the center of the beam. The green curve fixes two slits, the red curve fixes three, and the blue curve fixes four. The curves are normalized by area.

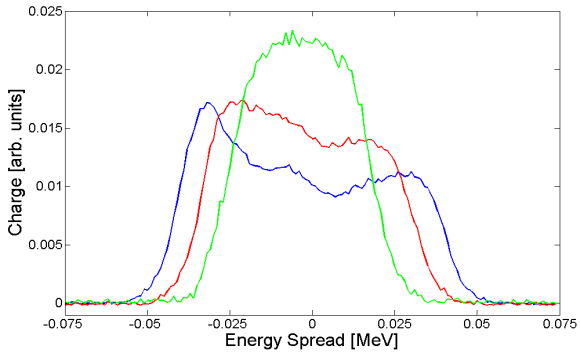

FIG. 6. Plots of partial projections on energy with three different beam currents. The green curve is from 20 mA, the red curve is from 30 mA, and the blue curve is from 40 mA. The correlation is more pronounced with increasing current, which indicates Coulomb forces cause the correlation. The curves are normalized by area.

the complex internal structure of the distribution visible on the partial projections.

The plots in Fig.5 show 1D partial projections with different numbers of fixed coordinates: the green line shows the energy spectrum measured with $x = x' = 0$ and integrated over y, y'; the red line shows the energy spectrum measured with $x = x' = y = 0$, integrated over y'; and the blue line shows the energy spectrum measured with $x = x' = y = y' = 0$. All three measurements are integrated over φ. The plots demonstrate the necessity of performing the scan in at least 4D for the correlation to become visible, and in 5D for resolving the details.

The plots in Fig.6 show 1D partial projections with 4 fixed coordinates $x = x' = y = y' = 0$ (all slits fixed at the beam center) measured for beam currents of 40mA, 30mA, and 20mA. The correlation is well pronounced at 40mA, becomes less visible with a smaller beam current of 30mA, and completely disappears at 20mA. This measurement convincingly demonstrates that the observed correlation is created by the Coulomb forces within the distribution.

While a precise simulation using the measured distribution is left for future work, a simple computer simulation is sufficient to elucidate the beam physics. A 1m long transport line consisting of drifts and four quadrupole magnets arranged similarly to the first 1m of the BTF beam line was simulated using PARMILA Particle-in-Cell code [22]. An ideal 6D Gaussian function was used to generate the initial particle coordinates. Partial projections on the $w - y'$ plane of the distribution function at the beam line exit are shown in Fig. 7 for two cases: a 10mA and a 100mA beam current. A pattern similar to the measurement in Fig. 3 is clearly visible only on the projection for high beam current, confirming that

Coulomb forces are responsible for creating this correlation in the 6D phase space distribution. Furthermore, it is interesting to note that reproducing the correlation in simulation does not require any novel or complex beam physics. In parallel with the experiment, the key is knowing to look at the partial rather than the integrated 2D projection (e.g., to maintain a high dimensional approach when viewing the lower dimensional subspaces). This reinforces the notion that the full 6D distribution is required for a complete understanding of the beam physics.

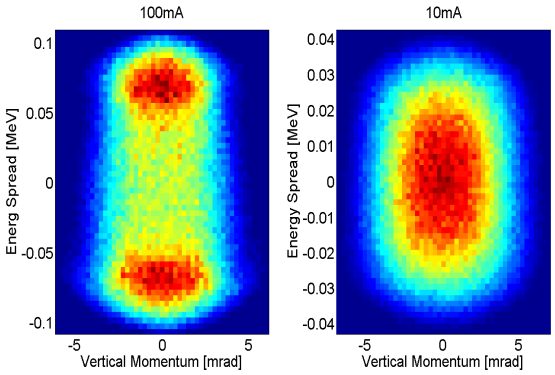

FIG. 7. Two plots of the partial projection of the energy spread, w, against the vertical momentum, y, for a 100mA (left) and a 10mA (right) simulated beam transport.

To conclude, the first full 6D phase space measurement of an accelerator beam has been completed. The measurement introduces a new field of experimental high dimensionality accelerator beam dynamics research. The high dimensionality scans showed a new correlation between degrees of freedom that are not typically measured together. These results indicate equation (1) is an invalid representation of the beam phase space distribution, and high dimensionality measurements are required to accurately represent the distribution. At present, the impact of the observed correlation on the beam evolution is unknown. This will be a topic of future work.

* The work at the University of Tennessee was supported by the U.S. National Science Foundation under grant PHY-1535312. ORNL is managed by UT-Battelle, LLC, under contract DE-AC05-00OR22725 for the U.S. Department of Energy.

† Also at Oak Ridge National Laboratory, Oak Ridge, Tennessee 37831, USA; mcousin2@utk.edu

[1] J Qiang, P L Colestock, D Gilpatrick, H V Smith, T P Wangler, and M E Schulze, "Macroparticle simulation studies of a proton beam halo experiment," PRSTAB **5**, 705–706 (2002).

[2] S Machida and R D Ryne, "Summary of session C: Space charge simulation and experiment," in *Proceedings of ICFA HB2004* (2004) p. 454.

[3] S Cousineau and I Hofmann, "Working session B summary: Space charge theory, simulations and experiments," in *Proceedings of ICFA HB2006* (2006) p. 363.

[4] A Aleksandrov, I Hofmann, and J-M Lagneil, "Summary report of the working group b: Beam dynamics in high intensity linacs," in *Proceedings of Hadron Beam 2008* (2008) p. 485.

[5] M Plum, Y Sato, and R Schmidt, "Summary of the working group on commissioning and operations," in *Proceedings of ICFA HB2012* (2012) p. 620.

[6] C K Allen, K C D Cha, P L Colestock, R W Garnett, J D Gilpatrick, W P Lysenko, J D Schneider, R L Sheffield, H V Smith, T P Wangler, J Qiang, K R Crandall, and M E Schulze, "Experimental study of proton beam halo in mismatched beams," in *Proceedings of LINAC2002* (2002) p. 395.

[7] S Nath, J Billen, J Stovall, H Takeda, L M Young, K Crandall, and D Jeon, "Particle-beam behavior in the sns linac with simulated and reconstructed beams," in *Proceedings of PAC2003* (2003) p. 1515.

[8] C. Xiao, M. Maier, X. N. Du, P. Gerhard, L. Groening, S. Mickat, and H. Vormann, "Rotating system for four-dimensional transverse rms-emittance measurements," Phys. Rev. Accel. Beams **19**, 072802 (2016).

[9] Eduard Prat, Masamitsu Aiba, Simona Bettoni, Bolko Beutner, Sven Reiche, and Thomas Schietinger, "Emittance measurements and minimization at the swissfel injector test facility," Phys. Rev. ST Accel. Beams **17**, 104401 (2014).

[10] T. P. Wangler, K. R. Crandall, R. Ryne, and T. S. Wang, "Particle-core model for transverse dynamics of beam halo," Phys. Rev. ST Accel. Beams **1**, 084201 (1998).

[11] V. Danilov, S. Cousineau, S. Henderson, and J. Holmes, "Self-consistent time dependent two dimensional and three dimensional space charge distributions with linear force," Phys. Rev. ST Accel. Beams **6**, 094202 (2003).

[12] H. R. Kremers, J. P. M. Beijers, and S. Brandenburg, "A pepper-pot emittance meter for low-energy heavy-ion beams," Rev. Sci. Instrum. **84**, 025117 (2013), arXiv:1301.3287 [physics.ins-det].

[13] V Yakimenko, M Babzien, I Ben-Zvi, R Malone, and X-J Wang, "Electron beam phase-space measurement using a high-precision tomography technique," Physical Review Special Topics-Accelerators and Beams **6**, 122801 (2003).

[14] D Stratakis, RA Kishek, H Li, S Bernal, M Walter, B Quinn, M Reiser, and PG OShea, "Tomography as a diagnostic tool for phase space mapping of intense particle beams," Physical Review Special Topics-Accelerators and Beams **9**, 112801 (2006).

[15] Michael Röhrs, Christopher Gerth, Holger Schlarb, Bernhard Schmidt, and Peter Schmüser, "Time-resolved electron beam phase space tomography at a soft x-ray free-electron laser," Physical Review Special Topics-Accelerators and Beams **12**, 050704 (2009).

[16] S. Hancock, Shane R. Koscielniak, and M. Lindroos, "Longitudinal phase space tomography with space charge," *Particle accelerator. Proceedings, 7th European Conference, EPAC 2000, Vienna, Austria, June 26-30, 2000. Vol. 1-3*, , 1726–1728 (2000).

[17] D Stratakis, RA Kishek, I Haber, RB Fiorito, JCT Thangaraj, K Tian, C Papadopoulos, M Reiser, and PG O'Shea, "Phase space tomography of beams with extreme space charge," in *Particle Accelerator Conference, 2007. PAC. IEEE* (IEEE, 2007) pp. 2025–2029.

[18] Gerald N Minerbo, OR Sander, and RA Jameson, "Four-dimensional beam tomography," IEEE Transactions on Nuclear Science **28**, 2231–2233 (1981).

[19] V Danilov and A Aleksandrov, "Beam invariants for diagnostics," in *Proceedings of EPAC2004* (2004) pp. 1518–1520.

[20] A Aleksandrov, M Champion, M Crofford, K Ewald, Y Kang, A Menshov, M Middenorf, S Murry, R Saethre, M Stockli, A Webster, R Welton, and A Zhukov, "Status of the new 2.5 mev test facility at sns," in *Proceedings of LINAC2014* (2014) p. 1105.

[21] A V Feschenko, "Methods and instrumentation for bunch shape measurements," in *Proceedings of PAC2001* (2001) p. 517.

[22] JH Billen and H Takeda, *PARMILA Manual*, Tech. Rep. (Report LAUR-98-4478, Los Alamos, 1998 (Revised 2004), 1998).